AIAA 81-4089

Critical Study of Calculations of Subsonic Flows in Ducts

Gino Moretti*
Polytechnic Institute of New York, Farmingdale, N. Y.
and
Maurizio Pandolfi†
Politecnico di Torino, Turin, Italy

The numerical treatment of computational boundaries drawn across regions of subsonic flow is discussed. The need for a physical model of the flow outside the boundaries, to assist time-dependent computations aimed at asymptotic steady states, is emphasized. Two different models to produce a subsonic source flow are studied and applied, reaching a very high accuracy.

I. Introduction

In the present paper, we discuss the numerical treatment of computational boundaries drawn across regions of subsonic flow. We will work out our arguments around the case of a subsonic source. At the boundaries, the number of unknowns n is greater than the number of equations m using information from interior points. From a bookkeeping viewpoint, it might seem that n-m physical parameters can be assigned arbitrarily. A time-dependent technique, however, generally does not tolerate such a simplistic approach and even if a steady state is reached asymptotically, the numerical evolution is not representative of any physical evolution.[1] A physical model of the flow outside the boundaries, furnishing n-m additional equations, should be adopted.

In what follows, we will consider a region of interest, limited by arbitrary, permeable boundaries. Such a possibility was not contemplated in Ref. 1, where it seemed that a problem in a region limited by subsonic boundaries could only be properly solved if the computational region were extended to infinity. Although conceptually correct, the procedure is impractical and lacks generality. Indeed, despite strong stretchings of coordinates, the number of computational mesh points has to be increased substantially. At a distance from the region of interest, resolution is, in any case, very poor; in the long run, numerical inaccuracies produced at a large distance will eventually propagate into the region of interest and deface the results. Finally, if the conditions outside the region of interest are not compatible with a simple, uniform flow at infinity (for example, because the flow is not homentropic), the device cannot be applied.

More personal work on the subject, and interesting contributions by other authors[2,3] brought us to conclude that computations within regions limited by subsonic boundaries can be performed, without having to stretch the region to infinity. Our basic ideas have been published in the open literature[4,5]; nevertheless, we decided to discuss the problem in detail again, since a certain confusion still seems to exist.[6] Occasionally, intolerable limits are reached, for example, when conclusions about physics are drawn from incorrect numerical procedures.[7]

Received July 24, 1980; revision received Nov. 3, 1980.

*Professor. Fellow AIAA.

†Professor.

II. Inseparability of Initial Conditions and Boundary Conditions

We will discuss time-dependent techniques for the numerical evaluation of steady state flows; such techniques consist of stepwise integration in time of the Euler equations for unsteady flow, starting from an assumed set of initial data and continuing until no appreciable variation in time occurs. If the computational region is limited by permeable subsonic boundaries, *their treatment has to be patterned on a physical model, consistent with the initial conditions.* We will try to clarify this concept, beginning with a quasi-one-dimensional example. Two methods will be considered, based on a different choice of initial conditions.

III. Quasi-One-Dimensional Problem

Let us consider a duct, the cross-sectional area of which increases along the x axis, and which has a finite length. It is known that, in the absence of viscosity and heat addition, a subsonic, steady flow in the duct is isentropic. If the stagnation values of pressure, density and temperature are taken as unity, the steady flow in the duct is uniquely determined by a single parameter, for example by the inlet Mach number or by the exit pressure.

If we want to evaluate such a steady flow using a time-dependent technique to solve the Euler equations of motion, we must, first of all, choose a set of initial conditions. An obvious rule of common sense should guide us to choose initial conditions which are as simple as possible and which can start an evolution having a physical meaning. For example, we can reformulate the problem by letting the duct accelerate from a state of rest to a cruising speed (first method), or we can open a diaphragm at the end section of the duct, assuming that the external ambient is at a pressure lower than the inside of the duct (second method).

First Method

Let us lay the duct along the x axis, so that its inlet section is at $-x_0$ and its exit section at x_0; then, let us attach two semi-infinite pipes to the duct, one to the inlet section and the other to the exit section. Each pipe has the same cross-sectional area as the section to which it is attached. By so doing, the length of the duct becomes infinite, and the original duct becomes a transition between two cylindrical pipes. Let us now assume that the duct is at rest, and the gas within it is also at rest. At time $t=0$, the entire duct is set into motion, for example toward the left, and it is accelerated until it reaches a cruising speed, V_0. An observer, moving with the duct, will believe that the gas at $\pm\infty$ is moving, from left to right, at a speed which is equal and opposite to the actual speed of the duct. Accordingly, and knowing the speed of sound of the gas at rest a_0 (which is the speed of sound at infinity), the observer defines a Mach number of the flow in the duct at $\pm\infty$, which we will denote by M_0.

The initial acceleration of the duct produces an expansion in the transitional region; the two fronts of the expansion propagate to the left and to the right with respect to the observer. The left front will eventually move at a speed $V_0 - a_0$. The gas velocity with respect to the observer, u, which is equal to V_0 at $-\infty$, increases behind the left front, because of the expansion. Correspondingly, the Mach number increases from left to right, in a region following the left perturbation front. In the transitional region, instead, the evolution of the flow is dominated by the variable geometry, which tends to slow down the flow, increasing its pressure. Here the pattern will quickly become steady. To the right, the expansion front will proceed at a speed equal to $V_0 + a_0$. At a given time, $t > t_0$ (where t_0 is the instant at which the acceleration stops), the pressure distribution along the duct will appear as in Fig. 1. There, points A and F are the perturbation fronts; the gas to the left of A and to the right of F is unperturbed, and its velocity is V_0. Point A moves to the left at the speed $V_0 - a_0$, point F moves to the right at the speed $V_0 + a_0$. Points B and E also move, to the left and to the right, respectively, but more slowly than A and F, so that the pressure gradients in AB and EF tend to flatten out. Such regions (AB and EF) are obviously regions of unsteady flow. Between B and E the flow is practically steady; this region of steady flow keeps growing in length, due to the motion of B and E. Between B and C, as well as between D and E, the pressure is asymptotically constant since the cross-sectional area is constant; between C and D, a steady compression takes place: the flow moves from left to right, against a positive pressure gradient. If the value of V_0 has been properly chosen, the flow in the transition has to be equal to the steady flow in the duct of finite length, as defined.

The asymptotic solution, composed of two unsteady flows bracketing a steady flow, can be determined without difficulty. Note, indeed, that, for $|x| > x_0$ and $t > t_0$, the duct is cylindrical and the frame of reference moves at a constant speed; therefore, the classical theory of one-dimensional, isentropic, unsteady flow holds. Since the flow to the left of A and the flow to the right of F are constant, both waves AB and EF are simple waves. If by a_- and a_+ we denote the speed of sound at any point between B and C and between D and E, respectively, the invariance of one of the Riemann parameters in each simple wave allows the following equations to be written:

$$a_- = a_0 \frac{1+\delta M_0}{1+\delta M_-}, \quad a_+ = a_0 \frac{1-\delta M_0}{1-\delta M_+} \tag{1}$$

where

$$\delta = (\gamma - 1)/2 \tag{2}$$

In the steady flow between B and E,

$$\frac{a_-}{a_+} = \left(\frac{1+\delta M_+^2}{1+\delta M_-^2}\right)^{1/2} \tag{3}$$

and

$$\frac{A_+}{A_-} = \frac{M_-}{M_+}\left(\frac{1+\delta M_+^2}{1+\delta M_-^2}\right)^{\frac{\gamma+1}{2(\gamma-1)}} \tag{4}$$

where A_- and A_+ are the inlet area and the exit area of the finite length duct, respectively. The above equations are four

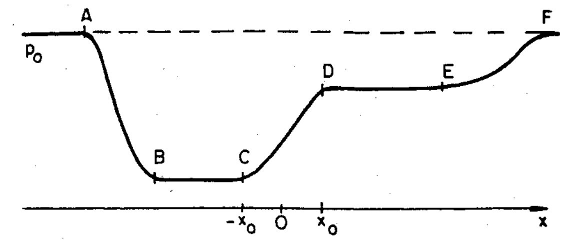

Fig. 1 Asymptotic pressure distribution in a duct.

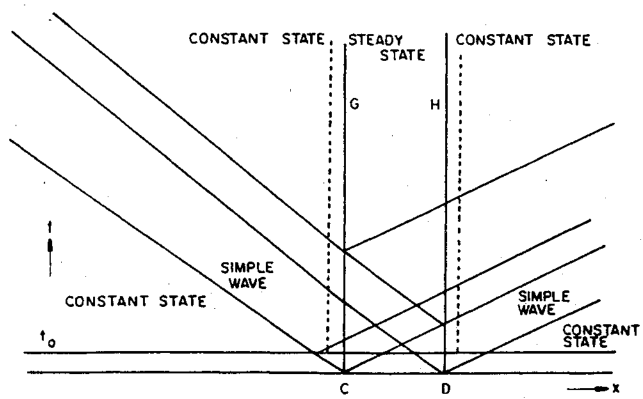

Fig. 2 Characteristic pattern for a duct in the model 1 flow.

equations for the five unknowns, M_0, M_-, M_+, a_- and a_+. Now, if we want to prescribe the inlet Mach number, M_-, Eq. (4) provides M_+, Eq. (3) provides a_-/a_+, and M_0 is easily obtained from the ratio of the two expressions of Eq. (1).

Typical characteristic patterns for subsonic flows are shown in Fig. 2. The geometrical transition occurs between the two vertical lines, CG and DH. Despite the complication of the initial perturbation, which occurs in a region of variable cross section and in an accelerating frame, we see that, as soon as the acceleration phase is over, *two arbitrary, fixed boundaries bracketing the transitional duct* (such as the ones indicated by dotted lines in Fig. 2) *are traversed by simple waves.*

Therefore, we can proceed as follows: With

$$P = \ln p, \quad T = p/\rho = \exp[(\gamma-1)P/\gamma] \tag{5}$$

the equations of motion, in a frame relative to the moving duct, are:

$$\begin{aligned} &P_t + uP_x + \gamma u_x + \gamma u A_x / A = 0 \\ &u_t + uu_x + TP_x + V_t = 0 \end{aligned} \tag{6}$$

where A is the cross-sectional area of the duct and the term V_t provides the change in momentum due to the acceleration of the duct.

The infinitely long duct is then mapped onto a finite length by a stretching function,

$$x = \frac{1}{2\alpha} \ln \frac{X}{1-X}, \quad X = 1 - \frac{1}{1+e^{2\alpha x}}, \quad X_x = 2\alpha X(1-X) \tag{7}$$

so that $X=0$ and $X=1$ correspond to $x=-\infty$ and $x=+\infty$, respectively.

The mapping is not necessary, strictly speaking, since the computational region is going to be truncated, as we will show below; but it is convenient in order to insure an optimal distribution of computational nodes, regardless of the total number of points taken into account. Consequently, the equations of motion in Eq. (6) become

$$P_t + X_x(uP_X + \gamma u_X) + \gamma u A_x / A = 0$$
$$u_t + X_x(uu_X + TP_X) + V_t = 0 \tag{8}$$

The equations of motion in the (X, t)-frame are then integrated using the MacCormack scheme[8]; derivatives of any function f with respect to X at any point whose abscissa is nX are approximated by

$$f_X \approx (f_{n+1} - f_n)/\Delta X \quad \text{at the predictor level}$$
$$\tilde{f}_X \approx (\tilde{f}_n - \tilde{f}_{n-1})/\Delta X \quad \text{at the corrector level} \tag{9}$$

Updating of any function f in time from the instant $k\Delta t$ to the instant $(k+1)\Delta t$ is performed as follows:

$$\tilde{f} = f^k + f_t \Delta t \quad \text{at the predictor level}$$
$$f^{k+1} = (f^k + \tilde{f} + \tilde{f}_t \Delta t)/2 \quad \text{at the corrector level} \tag{10}$$

The initial values (gas at rest) are defined as $P=0$, $u=0$, $T=1$ throughout. At $X=0$ and $X=1$, P is kept equal to 0 during the entire computation, and u is set equal to the velocity at infinity, V. The latter is defined as

$$V = -V_0 \sin\omega t \quad (t < t_0 = \pi/2\omega)$$
$$V = -V_0 \quad (t \geq t_0) \tag{11}$$

The value of Δt is defined, at every step, according to the CFL rule,[9] as

$$\Delta t = 0.8 \frac{\Delta x}{u+a} \tag{12}$$

where the factor 0.8 is introduced for the sake of safety. The temperature, T, is computed from Eq. (5). Updating of V_t occurs between the predictor and the corrector level.

To work out a practical example, we will define a unit length so that $x_0 = 0.5$. We will assume that the cross-sectional area grows linearly from $A_- = 1$ to $A_+ = 2$. We will define V_0 in order to have $M_- = 0.5$. We will spread a large number of computational nodes (typically, 101) between $x = -\infty$ and $x = +\infty$; but impose that the region of interest, between $-x_0$ and $+x_0$ is covered by 20 mesh intervals only (between the 40th and the 60th node, approximately). Such stipulations are automatically executed by the program, which determines V_0 once M_- and A_+/A_- are prescribed, and evaluates a correct value of α to accommodate the computational nodes as required. With $\omega = \pi/2$, say, few computational steps are needed to reach t_0; from that moment on, the computation is performed only between node 37 and node 63, so that only two stumps of the semi-infinite pipes, covered by two mesh intervals, are taken into consideration.

The values of P and u at boundary points could be computed, in principle, as

$$f^{k+1} = f^k + \frac{u \pm a}{x - x_1}(f_1^k - f^k)\Delta t \tag{13}$$

where $f = P$, u and the index 1 denotes values at the interior point next to the boundary. The lower and upper signs are used at the left and right boundary, respectively. This amounts to transferring the values of P and u, unchanged, to the initial and the final node from inside the first and the last interval, respectively, along the left-running characteristic in the former, and the right-running characteristic in the latter; the interpolation to obtain the values to be transferred is linear. The evaluation is correct, in principle, because no physical parameter changes along a straight characteristic in a simple wave. In practice, it works well in the problem described above but in other applications (for example, as discussed in Sec. IV) it may not work at all because of cumulative errors introduced in the successive interpolations between the boundary point and its neighbor. In Sec. IV, we will resume the argument and show how the simple wave concept can be rephrased with more flexibility and a wider range of validity.

We have chosen to describe the technique in connection with the MacCormack scheme for the sake of simplicity; the results presented below, however, have been obtained, with no difference in the first 5 significant digits, also when other predictor-corrector schemes of second-order accuracy were used, viz. the λ-scheme in its original form[10] and in Gabutti's variation,[11] and an interesting scheme, proposed independently by Zhu et al.[12] and recently brought to our at-

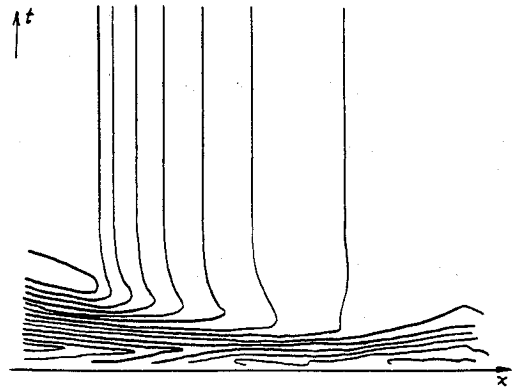

Fig. 3 Isobars pattern for a duct in the model 1 flow.

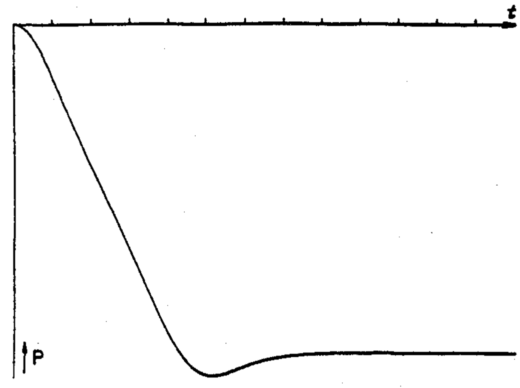

Fig. 4 Pressure variation at the inlet of a duct in the model 1 flow.

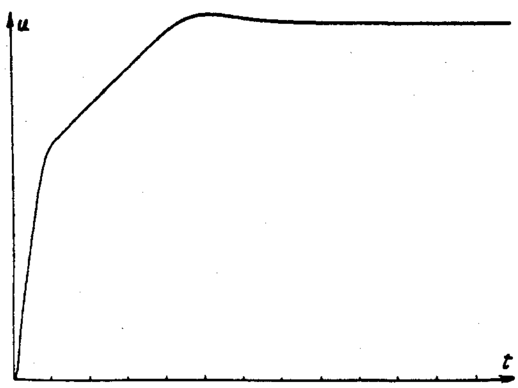

Fig. 5 Velocity variation at the inlet of a duct in the model 1 flow.

tention. In other words, in this case the importance of the integration scheme for interior points is overshadowed by the importance of the treatment of boundary points.

Results of the calculation in progress are shown in Fig. 3 by a set of isobars (values of P, spaced .02 apart) and in Figs. 4 and 5 by plots of P and u at the inlet, for the first 400 steps. It is evident that, at the end of the calculation, a well established steady state has been reached.

Second Method

We turn now to a different method for the numerical evaluation of the steady flow in the duct as the asymptotic state of a time-dependent evolution. We want to limit the calculation to the region of interest from the first computational steps; therefore, the computational region is always bounded by two x=constant lines through which the gas flows at a subsonic speed. Signals, thus, are permitted to traverse the lines in both directions. Purposely, we do not want to deal with a situation where the boundaries are traversed by simple waves. At every step in time, the signals from inside the region of interest travel outside and modify the surrounding ambient. Signals penetrating from the outside ambient carry information which is a consequence of the past history of the outside flow, which is essentially unknown. Consequently, we must substitute for it with a model capable, at least, of describing the effect of the outside evolution on the signal transmitted inside. Obviously, if the handling of the boundaries is not consistent with a physical model, spurious signals can penetrate the region of interest from outside; an asymptotic state may never be reached or, if reached, may be incorrect.

The equations of motion for a fixed, unstretched, (x, t)-frame are still Eq. (6), without the V_t term. Let stagnation pressure, density, and temperature be chosen as unity, so that the stagnation speed of sound is $\gamma^{1/2}$; Eq. (5) still holds. From these two equations we can obtain two compatibility equations along characteristics:

$$a(P_t+\lambda_2 P_x)+\gamma(u_t+\lambda_2 u_x)+\gamma auA_x/A=0 \tag{14}$$

$$a(P_t+\lambda_1 P_x)-\gamma(u_t+\lambda_1 u_x)+\gamma auA_x/A=0 \tag{15}$$

with

$$\lambda_1=u-a, \qquad \lambda_2=u+a \tag{16}$$

The first equation holds along the right-running characteristic, the second equation along the left-running characteristic. At the inlet section, Eq. (15) is usable because it carries information from inside, but Eq. (14) must be substituted with another condition.

In order to obtain a condition consistent with a physical model, we can imagine that the flow comes from an infinite capacity, where the stagnation conditions are known. The transition from the infinite capacity to the inflow boundary can be conceived as occurring by means of a convergent nozzle, whose length is vanishingly small, so that *the flow through it can be considered as steady*. Under such assumptions, pressure and velocity are related by the equation:

$$P=\frac{\gamma}{\gamma-1}\ln\left(1-\frac{\gamma-1}{2\gamma}u^2\right) \tag{17}$$

At the inlet itself, P and u are functions of time, but Eq. (17) is valid at every instant of time through the hypothetical nozzle, of which the inlet is the last section. Therefore, Eq. (17) can be differentiated in time, yielding

$$TP_t=-uu_t \tag{18}$$

This equation can be used in conjunction with Eq. (15) to determine the rate of change in time of *both* P and u. Following de Neef,[13,14] one can first compute the increments in P and u, ΔP^E and Δu^E, at the inflow boundary, by integrating the Euler equations and using only information from the interior of the region. Since both these increments and the exact increments, ΔP and Δu, satisfy the same compatibility Eq. (15), we can write:

$$a(P_t+\lambda_1 P_x)-\gamma(u_t+\lambda_1 u_x)+\gamma uaA_x/A=0$$

$$a(P_t^E+\lambda_1 P_x)-\gamma(u_t^E+\lambda_1 u_x)+\gamma uaA_x/A=0$$

By subtraction,

$$a(P_t^E-P_t)-\gamma(u_t^E-u_t)=0 \tag{19}$$

From Eqs. (18) and (19), the correct change in u, Δu, is obtained as

$$\Delta u=-\frac{a(a\Delta P^E-\gamma\Delta u^E)}{\gamma(u+a)} \tag{20}$$

Once the new value of u is found, the new value of P is easily determined from Eq. (17).

At the outflow boundary, one can develop similar arguments. In a general problem, though, the stagnation pressure is not a constant and it is not necessarily equal to the inlet stagnation pressure, due to the formation of shocks; therefore, Eq. (17) should not be used. We will use here another physical model, assuming that the duct opens into an infinite capacity, where the pressure, p_∞, is prescribed. In a one-dimensional problem, the exit pressure can be made equal to p_∞, and only the velocity remains to be computed. To this effect, Eq. (14), relating P and u along the right-running characteristic, can be used.

A calculation based on the same geometry as in the preceding section has been performed. The downstream pressure was prescribed to produce an inlet Mach number equal to 0.5. The MacCormack scheme was used, but the endpoints were computed with second-order accuracy by using, in one of the two levels at each step, the three-point approximation explained in Ref. 10. The region of interest was divided into 20 intervals. Initially, both P and u were set equal to zero everywhere except at the outlet, where the pressure is given its prescribed downstream value. In other words, the calculation is started from a state of rest, simulating the abrupt opening of a diaphragm at the outlet. The evolution is rather complicated; a wave proceeds from the outlet to the inlet but, when it reaches it, neither the pressure nor the velocity can be brought to their steady values. The wave is partially reflected back; the reflected wave reaches the outlet and another similar cycle starts. At every cycle, the inlet values get closer and closer to their steady state determinations, but the process is time-consuming; eventually, the long waves are replaced by ripples which require a long time to be completely damped out.

The evolution appears as described in Fig. 6, which shows isobars in the (x,t)-plane. Note the difference between the initial waves and the gentle ripples in the second half of the calculation. The effect of the waves on the inlet pressure and velocity is clearly shown by Figs. 7 and 8, where such parameters are plotted as functions of time. The calculation uses 20 intervals along the duct, and it has been carried on for 2500 steps.

IV. Concluding Remarks on One-Dimensional Problems

From the preceding exercises we have learned that there are at least two different possible ways of computing a quasi-one-dimensional, subsonic, steady flow by a time-dependent

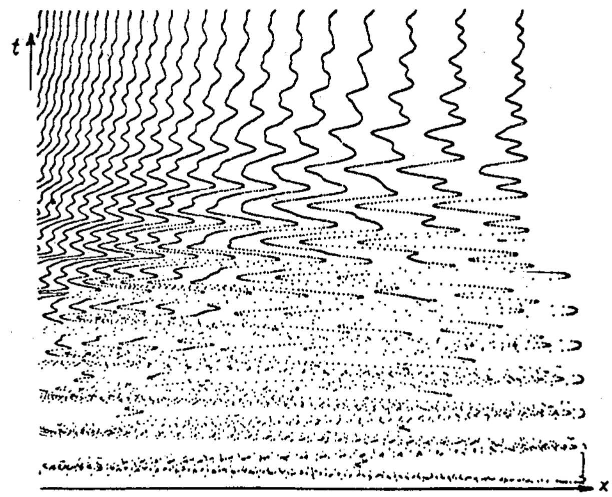

Fig. 6 Isobars pattern for a duct in the model 2 flow.

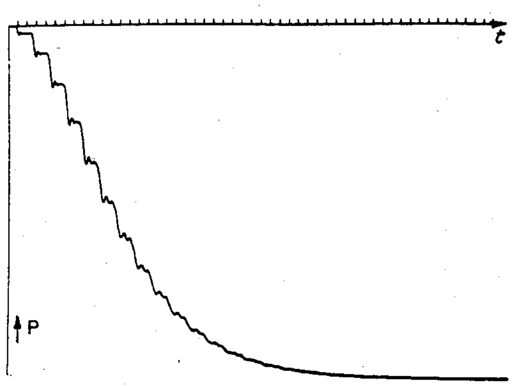

Fig. 7 Pressure variation at the inlet of a duct in the model 2 flow.

technique:

1) By accelerating the duct from rest, after having attached two semi-infinite pipes to the inlet and outlet of the duct; in this case, at the end of the acceleration stage, the pipes can be shortened and the boundaries evaluated using a simple wave concept; or

2) By opening a diaphragm at the duct outlet and letting the flow develop; in this case, the inlet can be evaluated using a left-running characteristic and imposing a constant value of the stagnation pressure, and the outlet using a right-running characteristic and imposing a constant value of the pressure in a fictitious infinite capacity into which the duct is assumed to discharge.

The arguments presented in the previous section and our numerical results show that both procedures are equally sound; but a few comments may help to sharpen the picture.

One may ask: Would it be possible to use the boundary technique of the first type together with the initial conditions of the second type, or vice versa? The answer is positive, provided that one proceeds with caution. As we said in Sec. II, the physical model expressed by our treatment of boundary conditions must be consistent with the initial conditions. For a given set of initial conditions, different treatments of the boundaries correspond to different physical models. Only one of them will be equivalent to the real phenomenon which we are trying to evaluate; all other models will provide solutions of different problems and, consequently, will be inadequate for our goal.

In the first method described above, the "simple wave" treatment is physically correct. It does, indeed, prescribe that no signals are sent from the outside into the region of interest; and this may occur only when no signals are generated outside. In an inviscid flow, even if the walls are accelerated, no

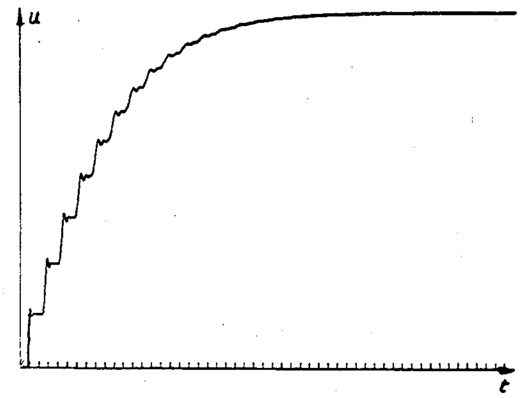

Fig. 8 Velocity variation at the inlet of a duct in the model 2 flow.

perturbation is created by a cylindrical pipe. *All the necessary elements to define the steady flow in the duct are generated, within the duct itself, during the acceleration process.* Note that in our example the inlet Mach number was specified; from it the cruising speed of the duct and, consequently, the inlet stagnation pressure were deduced; the outlet pressure was obtained as a consequence of the time-dependent calculation. If the latter had to be prescribed in advance, in terms of the inlet stagnation pressure (which is not the pressure of the gas at rest), one could easily obtain M_+ and then proceed as indicated in Sec. III, interchanging the role of M_+ and M_-.

A boundary treatment of the second type could be applied to initial conditions of the first type, but the application is not straightforward. In fact, one must first determine the stagnation temperature of the gas, T_0, in region BC (Fig. 1), since this is the value pertinent to the steady flow. By using the first of Eq. (1) and

$$a_{0-}^2 = a_-^2 \,(1+\delta M_-^2)$$

and replacing Eq. (17) with

$$T = T_{0-}\,\left(1-\frac{\gamma-1}{2\gamma}u^2\right)$$

it can be seen that Eq. (18) has to be replaced by

$$TP_t = -\left(\frac{1+\delta M_0}{1+\delta M_-}\right)^2 (1+\delta M_-^2)\,uu_t \tag{21}$$

In the second approach, the motion is started by the opening of a diaphragm at the end of the duct; and the air supply is assumed to be provided by an infinite capacity containing gas at rest. All perturbations generated inside must interact with the reservoir upstream; therefore, the inlet boundary cannot be made impermeable to incoming signals. Nevertheless, a "simple wave" concept can be used at the upstream boundary if we change the model, by substituting the infinite capacity with a semi-infinite pipe. In this case, the opening of a diaphragm at the downstream boundary generates an expansion wave which travels upstream and which becomes a simple wave within the pipe. A stump of the pipe, containing not more than three computational nodes, can be used, and "simple wave" concepts applied to the calculation of the inlet boundary point, whereas at the outlet boundary point the pressure can be prescribed as in the second method of Sec. III. The procedure described in connection with Eq. (13), however, cannot be used. We will rephrase it in a different form.

The equations for the two Riemann invariants at the inlet are:

$$a+\delta u=a_0, \qquad a-\delta u=a_*-\delta u_* \tag{22}$$

where the values denoted by * are interpolated between the first two nodes as in Eq. (13). Therefore,

$$a=(a_0+a_*-\delta u_*)/2, \quad u=(a_0-a_*+\delta u_*)/(\gamma-1) \tag{23}$$

As we said in Sec. III, in a simple wave, $a=a_*$ and $u=u_*$, so that the second of Eq. (22) is identically satisfied and the first is not needed. Numerically, to use such an assumption is very dangerous; any numerical inaccuracy in the first mesh interval is carried to the boundary point, whose determination has been made to depend on the interior values only. In the first example, there is no hint of danger because the acceleration process leads naturally to a smooth variation of physical parameters near the inlet boundary, with a negative pressure gradient and a positive velocity gradient. In the application of the simple wave concept to the second example, the waves travelling upstream may arrive with opposite gradients, due to geometry effects which are still felt, numerically, two nodes away from the beginning of the duct. As a result, the computed flow, after the arrival of the first perturbation, tends to degenerate, until eventually it is brought to a standstill.

A very important conclusion can be drawn: *Whatever the physical model for the exterior* (for example, infinite capacity or infinite pipe), *its influence on the interior, through the boundary, must be accounted for* (in the new simple wave model this is accomplished by Eqs. (23), which contain a_0).

To summarize: the first method allows the asymptotic values to be reached much faster than the second. The reason for it is simple: in the first case the entire length of the duct is affected by the acceleration process, simultaneously, whereas in the second case we must allow the complicated wave interplay described above to happen, and the elimination of residual ripples is a long process. Therefore, the first method should be applied whenever possible, using Eq. (23) at the inflow boundary. The second method, however, is more general. Arbitrary initial conditions can be imposed to simulate other transients, and models different from the infinite capacity or the semi-infinite pipe can be used, if necessary. Extension of the second model to two-dimensional problems is possible, as we will see in the next section.

Finally, let a word be said about imposing the exact values of all physical parameters at the boundaries. It can be seen that, even if the initial values are exact, the computed values tend to degenerate somewhat and wiggles develop, if the values of P and u are kept constant at the boundaries (Fig. 9). The phenomenon occurs because the solution of the partial differential equations and the solution of the finite difference equations cannot be identical, due to the presence of truncation errors in the former. Small discrepancies must be permitted at all nodal points, and the concept of accuracy is based on the order of magnitude of such discrepancies, not on their disappearance. Exact values imposed at one point do not yield to a proper distribution of truncation errors, and the neighboring points are affected. Such a behavior seems not to be well known and many authors[6,7] believe that overspecifying exact conditions at the boundaries is necessary to obtain a correct solution. Obviously, if this were the case, most of the problems of practical interest could not be solved numerically; knowledge of the exact solution at the boundaries, indeed, implies that the exact solution is known.

Once more, we stress that *the boundaries must be allowed to interplay with the waves which reach them.* The approximation in a numerical discretized solution is not exactly consistent with the exact values; waves, generated by truncation errors, must be left free to interact with the boundaries. Otherwise, a solution will be reached in which such truncation errors become mutually stabilized by the presence of local wiggles (which are obviously dependent on the mesh).

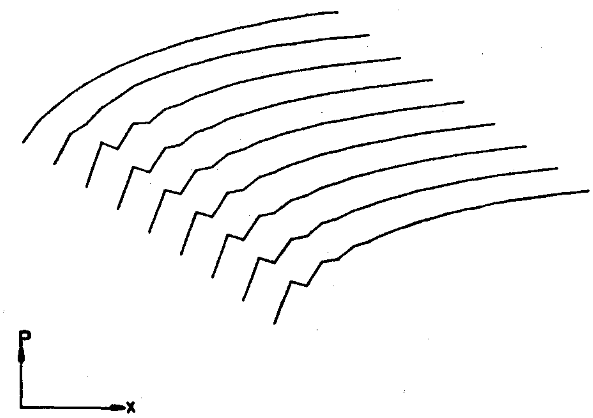

Fig. 9 Successive pressure patterns obtained starting from the exact solution and enforcing exact values at the boundaries.

V. Two-Dimensional Problems

In two-dimensional problems, there is more need for flexibility in defining upstream and downstream conditions than in one-dimensional cases. For example, the incoming flow may not be homentropic. Besides, problems of flows in ducts and problems in infinite domains suggest different ways of modeling artificial boundaries. In the present paper, we will limit ourselves to the former case, where the second method of solution seems to be more appropriate for a generalized extension.

The computation is best performed in a computational plane, defined by coordinates X and Y, which are orthogonal. The computational region is a rectangle; in a duct problem, two opposite sides of the rectangle are the images of the rigid boundaries of the duct, and the other two opposite sides are the images of the inlet and outlet cross-sections, respectively. The grid lines in the physical space are generally not orthogonal.

For the sake of simplicity, we consider a duct with straight walls, defined by $y/x=\pm\alpha$, between $x=1$ and $x=2$. A computational grid is defined by the transformation:

$$X=x, \qquad Y=\frac{y}{\alpha x} \tag{24}$$

In the (X, Y, t) space, the equations of motion are

$$P_t+uP_X+BP_Y+\gamma u_X+\gamma Y_x u_Y+\gamma Y_y v_Y=0$$
$$u_t+uu_X+Bu_Y+TP_X+TY_xP_Y=0$$
$$v_t+uv_X+Bv_Y+TY_yP_Y=0$$
$$S_t+uS_X+BS_Y=0 \tag{25}$$

with

$$B=uY_x+vY_y, \quad Y_x=1/\alpha x, \quad Y_y=-Y/x$$

The use of Cartesian x and y, as well as of the corresponding velocity components, u and v, is not the most appropriate for the problem but it is useful for the following discussion.

As in the one-dimensional problem, we will integrate Eq. (25) using the MacCormack scheme, modified by three-point operators at boundary points. The line $y=0$ $(Y=0)$ is a symmetry line. At points on the rigid wall, $Y=1$, the values are first computed using the MacCormack scheme. Then they are corrected to satisfy the boundary condition, which prescribes the vanishing of the normal velocity component, V_n:

$$V_n=v\cos\alpha-u\sin\alpha=0 \tag{26}$$

Following de Neef again,[13] an equation similar to Eq. (19) can be written:

$$a(P^E - P) + \gamma(v^E \cos\alpha - u^E \sin\alpha) = 0 \tag{27}$$

and the correct value of P can be evaluated from it. The u-component is accepted from the general integration procedure, since it is dominated by derivatives taken along the wall, and then v is computed from Eq. (26).

At the inlet, we prescribe the stagnation pressure P_0, the slope of the velocity vector, $\sigma = v/u$, and the entropy at each mesh point. According to our previous discussion, the use of stagnation pressure is correct. The entropy must always be prescribed; in fact, it is carried by the particles of the incoming flow, regardless of its evolution within the duct. The choice of σ for a ducted flow corresponds to a reasonable, experimentally reproducible condition. It is not, however, the only possible choice for other problems. For example, in a cascade problem, the angular velocity may have to be prescribed and from it u and, consequently, the incidence, will follow. Naturally, stagnation pressure as well as entropy can be prescribed with different values at each boundary point. In the present case, we will consider the flow to be homentropic; therefore, the stagnation pressure will also be a constant.

In the spirit of the second method of Sec. III, and having prescribed $\sigma = y$, we can easily see that Eq. (18) must be replaced by

$$TP_t = -(1 + y^2)uu_t \tag{28}$$

and Eq. (20) by

$$\Delta u = -\frac{a(a\Delta P^E - \gamma \Delta u^E)}{\gamma[(1+y^2)u + a]} \tag{29}$$

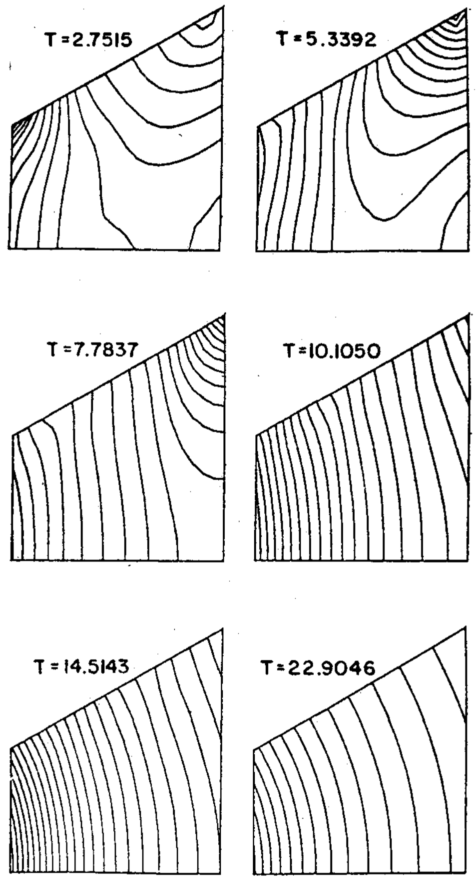

Fig. 11 Typical isomachs at successive times in a two-dimensional duct.

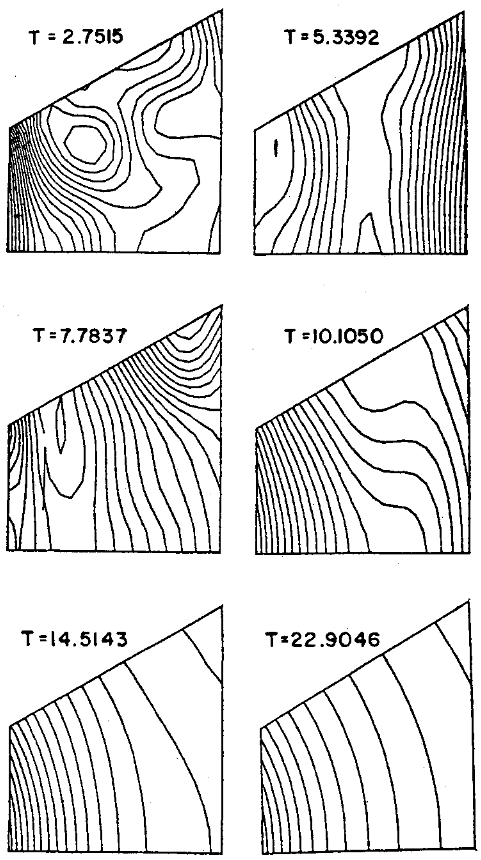

Fig. 10 Typical isobars at successive times in a two-dimensional duct.

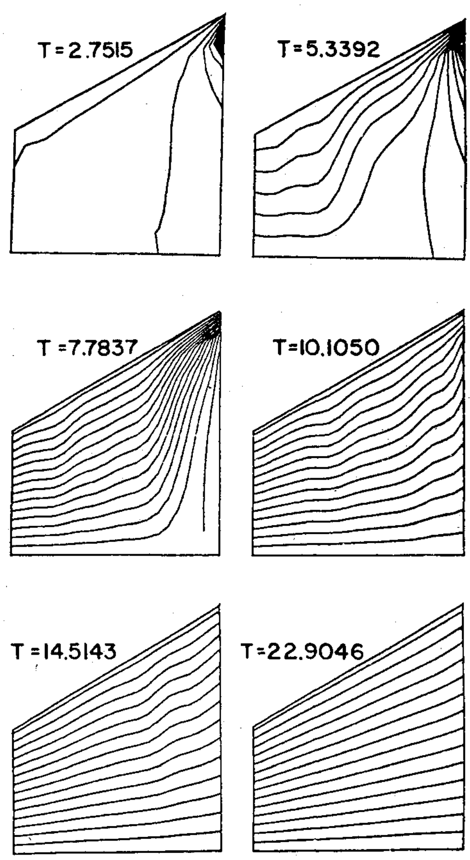

Fig. 12 Typical lines of constant velocity slope at successive times in a two-dimensional duct.

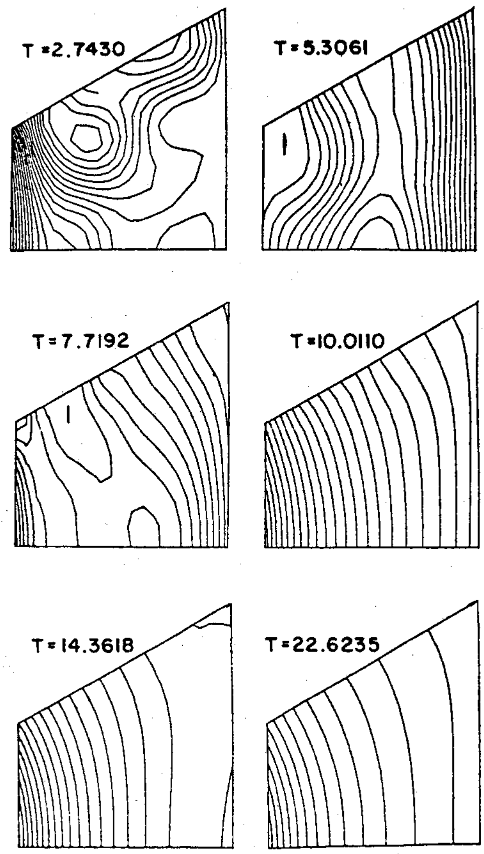

Fig. 13 Typical isobars at successive times in a two-dimensional duct, with pressure constant across the outlet.

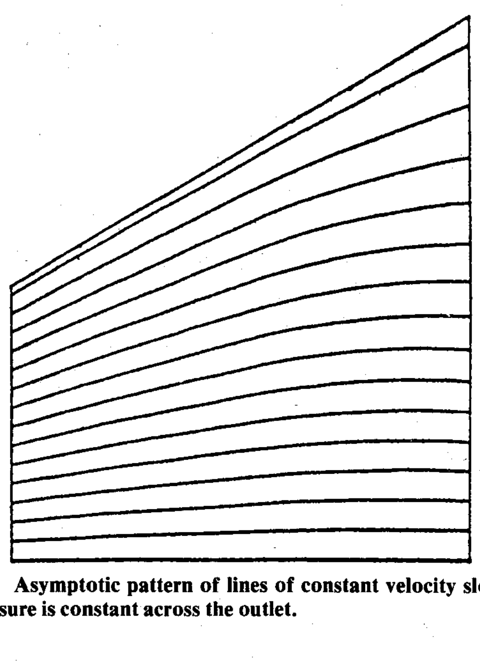

Fig. 14 Asymptotic pattern of lines of constant velocity slope when the pressure is constant across the outlet.

Once the new value of u is found, v follows from $v=yu$ and P from

$$P=\frac{\gamma}{\gamma-1}\ln\left[1-\frac{\gamma-1}{2\gamma}(u^2+v^2)\right] \tag{30}$$

At the outlet, we imagine that the flow at each boundary point continues as a jet, which asymptotically has a given direction (σ_∞) and a given pressure (P_∞). No other values can be specified. Indeed, the entropy is carried to the boundary from within and a study of the v-momentum equation[15] shows that the numerical domain of dependence of v must be confined to points within the computational region or on the boundary.

Therefore, at each point we write the continuity equation,

$$\rho u=\rho_\infty u_\infty \tag{31}$$

the energy equation,

$$T+\frac{\delta}{\gamma}(u^2+v^2)=T_\infty+\frac{\delta}{\gamma}u_\infty^2(1+\sigma_\infty^2) \tag{32}$$

and the counterpart of Eq. (19) at the outlet,

$$aP_t+\gamma u_t=aP_t^E+\gamma u_t^E=R \tag{33}$$

Taking into account that, in the present case, the flow is homentropic and, consequently, $d\rho/dP=\rho/\gamma$, $dT/dP=(\gamma-1)T/\gamma$, and letting $r=\rho_\infty/\rho$, we obtain from Eqs. (31) and (32):

$$uP_t+\gamma u_t=\gamma r u_{\infty t}$$

$$TP_t+uu_t=-vv_t+u_\infty u_{\infty t}(1+\sigma_\infty^2) \tag{34}$$

From these two equations, P_t and u_t can be obtained and replaced into Eq. (33), from which $u_{\infty t}$ and, consequently, Δu_∞ are obtained:

$$\Delta u_\infty=\frac{v\Delta v+(u+a)R/\gamma}{ra+u_\infty(1+\sigma_\infty^2)} \tag{35}$$

Again, Eqs. (34), multiplied by Δt, provide ΔP and Δu.

The first phase of the evolution of the flow is shown in Figs. 10-12 which present sequences of isobars, isomachs and lines of constant σ, respectively. The computational mesh contains 20 intervals in the x direction and 10 intervals in the y direction. The flow starts from rest, following the opening of a diaphragm at the outlet. The values of P_∞ are the exact values for a subsonic source flow having a Mach number equal to 0.5 in the lower point of the inlet. The flow is well stabilized after 1000 computational steps. At that stage, the maximum error in stagnation pressure over the entire region is 0.13%.

Another calculation has been made, assuming that P_∞, instead of being equal to the exact value across the outlet, was a constant, equal to the exact value at the lower point of the outlet. The sequence of isobars at successive times is shown in Fig. 13. The initial phase is not remarkably different from the initial phase shown in Fig. 10; the steady state, attained after 1000 steps, however, shows some interesting different features. In Fig. 14, one can see the effect that the new pressure distribution has on the shape of the lines of constant σ. Note that the result shown in Fig. 14 is obtained despite having imposed the same value of σ_∞ as in the previous case.

As far as stability of the calculation is concerned, it is clear that one steady solution or another is reached, according to the initial state and the model chosen to simulate upstream and downstream conditions, if such conditions are physically consistent with a steady flow. Effects such as separation and the onset of turbulence, which are typical of viscous flows and which are claimed to be found numerically in Ref. 7, do not appear in our results, based on a strictly inviscid model.

References

[1]Moretti, G., "Importance of Boundary Conditions in the Numerical Treatment of Hyperbolic Equations," *Physics of Fluids Supplement II*, 1969, pp. 13-20.

[2]Abbett, M. J., "The Steady Flow in a Two-dimensional DeLaval Nozzle as the Asymptotic Time Limit of an Unsteady Flow," in

Edelman, R. B. et al., "Some Aspects of Viscous Chemically Reacting Moderate Altitude Exhaust Plumes," Final Rept., Contract NAS8-21264, GASL, Westbury, N. Y., 1970.

[3]Serra, R. A., "Determination of Internal Gas Flows by a Transient Numerical Technique," *AIAA Journal*, Vol. 10, 1972, pp. 603-611.

[4]Pandolfi, M. and Zannetti, L., "Some Permeable Boundaries in Multidimensional Unsteady Flows," *Lecture Notes in Physics*, Vol. 90, (*Proceedings Sixth International Conference on Numerical Methods in Fluid Dynamics*), 1978, pp. 439-446.

[5]Pandolfi, M. and Zannetti, L., "Some Tests on Finite Difference Algorithms for Computing Boundaries in Hyperbolic Flows," *Notes on Numerical Fluid Mechanics*, Vol. 1 (Boundary Algorithms for Multidimensional Inviscid Hyperbolic Flows), edited by K. Förster, Vieweg Publishers, 1978, p. 68.

[6]Griffin, M. D. and Anderson, J. D., Jr., "On the Application of Boundary Conditions to Time Dependent Computations for Quasi-One-dimensional Fluid Flows," *Computers and Fluids*, Vol. 5, 1977, pp. 127-137.

[7]Cline, M. C., "Stability Aspects of Diverging Subsonic Flow," *AIAA Journal*, Vol. 18, 1980, pp. 534-539.

[8]MacCormack, R. W., "The Effect of Viscosity in Hypervelocity Impact Cratering," AIAA Paper 69-354, 1969.

[9]Courant, R., Friedrichs, K. O. and Lewy, H., "Ueber die partiellen Differenzleichungen der mathematischen Physik," *Mathematische Annalen*, Vol.100, 1928, pp. 32-74.

[10]Moretti, G., "The λ-Scheme," *Computers and Fluids*, Vol. 7, 1979, pp. 191-205.

[11]Gabutti, B., private communication, Universita di Torino, 1978.

[12]Zhu, Y., et al., "Difference Schemes for Initial-Boundary Value Problems of Hyperbolic Systems and Example of Application," *Scientia Sinica* (Special Issue II), 1979, p. 261.

[13]de Neef, T., "Treatment of Boundaries in Unsteady Inviscid Flow Computations," Rept. LR 262, Delft University of Technology, 1978.

[14]de Neef, T. and Moretti, G., "Shock Fitting for Everybody," *Computers and Fluids*, Vol. 8, 1980.

[15]Pandolfi, M. and Zannetti, L., "A Physical Approach to Solve Numerically Complicated Hyperbolic Flow Problems," *VII International Conference on Numerical Methods in Fluid Dynamics*, June 1980.